Extended data

Supplementary Figure legend

Supplemental Figure 1. Lactylation mediates CRC tumor development, related to Figure 1.

(**A**) Gene set enrichment analysis (GSEA) of TCGA-COAD dataset was performed to evaluate changes in glycolysis in CRC tumors and normal specimens. ES = 0.3875, NP=0.0316. (**B**) Immunohistochemical (IHC) staining was used to assess lactylation levels in a tissue microarray. (**C**) Western blotting was used to assess the expression of Pan Kla in tumor and normal specimens; T, tumor; N, normal. (**D**) The UMAP plot of clustered single-cell RNA-seq datasets demonstrates the existence of distinct CRC tumor subpopulations. The cells were clustered into eight different groups, with each cell cluster labeled and colored according to its subcellular type. (**E**) Western blot analysis was performed to assess the expression of CD133, Pan-Kla, Nanog, and OCT4 in CRC sphere and adherent cells. (**F**) Western blot was used to assess the expression of H4K12la in tumor and normal specimens; T, tumor; N, normal. (**G**) A schematic diagram illustrating sphere cell sorting. (**H**) Western blot analysis was performed to evaluate the expression of CD133, Pan Kla, Nanog and H4K12la in $CD133^-$ and $CD133^+$ cells.

Supplemental Figure 2. Lactate regulates the histone lactylation and stemness of CCSCs.

(**A**) Western blot analysis was performed to determine the expression of CD133, Nanog, Pan Kla, and H4K12la in SW-620 CSCs treated with lactate for 24 hours. (**B**) Western blot analysis was performed to evaluate the expression of CD133, Nanog, Pan Kla, and H4K12la in SW-620 CSCs treated with NALA for 24 hours. (**C**) Western blot analysis was performed to assess the expression of CD133, Nanog, Pan Kla, and H4K12la in

SW-620 CSCs cultured in regular medium containing varying concentrations of glucose for 24 hours; Right: Intracellular lactate levels were measured. (**D**) IF staining was performed to observe H4K12la (red) in LoVo cells treated with lactate for 24 hours. Scale bar: 100 μm. (**E**) HCT-116 CSCs were exposed to 2-DG for 24 hours. Left: Western blot analysis was used to assess the expression of CD133, Nanog, Pan Kla, and H4K12la; Right: Intracellular lactate levels were measured. (**F**) SW-620 CSCs were cultured under hypoxic conditions for different durations. Left: Western blot analysis was used to assess the expression of CD133, Nanog, Pan Kla, and H4K12la; Right: Intracellular lactate levels were measured. (**G**) The expression of LDHA was analyzed in the TCGA-COAD and TCGA-READ datasets (normal=51, tumor=647). (**H**) Kaplan-Meier overall survival analysis of LDHA expression in the public colorectal cancer dataset (GSE17536) (n=177, Cox regression analysis). $p < 0.001$.

Supplemental Figure 3. p300 is an H4K12la lactylase and HDAC1 is an H4K12la delactylase.

(**A**) Western blot analysis was used to evaluate the expression of p300, CD133, Pan-Kla, Nanog, Pan Ac, and H4K12la in siP300 SW-620 CSCs. (**B**) IF assay was performed to assess the expression of H4K12la and Pan Ac in siP300 SW-620 CSCs. Scale bar: 200 μm. (**C**) Western blot analysis was used to evaluate the expression of HDAC1, CD133, Pan-Kla, SOX2, Pan Ac, and H4K12la in shHDAC1 HCT-116 CSCs. (**D**) IF assay was performed to assess the expression of H4K12la and Pan Ac in shHDAC1 HCT-116 CSCs. Scale bar: 100 μm. (**E**) Western blot analysis was used to assess the expression of CD133, Pan Kla, Nanog, Pan Ac, and H4K12la in LoVo and SW-620 CSCs cultured in regular medium containing TSA for 24 hours. (**F**) Western blot analysis was used to assess the expression of CD133, Pan Kla, Nanog, Pan Ac, and

H4K12la in HCT-116 CSCs overexpressing HDAC1.

Supplemental Figure 4. Inhibition of lactylation makes CCSCs responsive to chemotherapeutic agents, related to Figure 4.

(**A**) Cell viability was assessed in SW-620 and LoVo CSCs treated with glucose and oxaliplatin for 24 hours. (**B**) Representative immunohistochemical images of H4K12la and Ki67 in tumor sections are shown. Scale bar, 50 μm. (**C**) Representative images of immunohistochemical staining for H4K12la and Ki67 in tumor sections. Scale bar, 50 μm. Three biological replicates were shown. The presented data shown represent the mean ± SD. Statistical analyses were performed using the Student's t-test. *$p < 0.05$, **$p < 0.01$.

Supplemental Figure 5. Ferroptosis in CCSCs is inhibited by histones lactylation.

(**A**) Cluster analysis of RNA expression levels in LoVo CSCs treated with oxaliplatin or oxaliplatin plus lactate. (**B**) KEGG enrichment analysis was conducted to identify the 20 most enriched KEGG terms, including ferroptosis. (**C** and **D**) Relative lipid ROS and MDA levels were tested in SW-620 CSCs treated with RSL3 (5 μM) or Erastin (5 μM) or oxaliplatin (5 μM) for 12 hours (n=3). (**E** and **F**) Relative levels of lipid ROS and MDA were measured in SW-620 CSCs treated with oxaliplatin (5 μM) and lactate for 12 hours (n=3). (**G** and **H**) Relative levels of lipid ROS and MDA were measured in LoVo CSCs treated with oxaliplatin (5 μM) and NALA for 12 hours (n=3). (**I** and **J**) Relative levels of lipid ROS and MDA were tested in SW-620 CSCs treated with oxaliplatin (5 μM) and NALA for 12 hours (n=3). (**K** and **L**) Relative levels of lipid ROS and MDA in were measured HCT-116 CSCs treated with oxaliplatin (5μM) and 2-DG for 12 hours (n=3). Three biological replicates were shown. The presented data show the mean ± SD; Comparisons were conducted using one-way ANOVA with

Tukey's test. *$p < 0.05$, **$p < 0.01$, ***$p < 0.001$. ns indicates no significant difference.

Supplemental Figure 6. Ferroptosis is inhibited by histone lactylation in CCSCs.

(**A** and **B**) Relative levels of lipid ROS and MDA were measured in shLDHA SW-620 CSCs treated with oxaliplatin (5 μM) for 12 hours (n=3). (**C** and **D**) Relative levels of lipid ROS and MDA were measured in siP300 SW-620 CSCs treated with oxaliplatin (5 μM) for 12 hours (n=3). (**E** and **F**) Relative levels of lipid ROS and MDA were measured in shHDAC1 HCT-116 CSCs treated with oxaliplatin (5 μM) for 12 hours (n=3). Three biological replicates were shown. The presented data show the mean ± SD; Comparisons were conducted using one-way ANOVA with Tukey's tes. *$p < 0.05$, **$p < 0.01$, ***$p < 0.001$.

Supplemental Figure 7. Expression of GCLC is transcriptionally activated by histone lactation.

(**A**) The H4K12la modification is primarily enriched at the TSS. (**B**) Genome-wide distribution of H4K12la- associated peaks in LoVo CSCs. (**C**) GCLC expression was analyzed in TCGA-COAD and TCGA-READ datasets: normal = 51, tumor = 647; ***p < 0.001.(**D**) CUT&Tag-qPCR assay was used to analyze H4K12la in the GCLC genomic region of SW-620 CSCs. (**E**) Quantitative real-time PCR (qPCR) analysis of GCLC mRNA levels in LoVo and SW-620 CSCs cultured in regular medium containing NALA for 24 hours (n=3). (**F**) Western blot analysis was used to assess GCLC expression in LoVo and SW-620 CSCs cultured in regular medium containing NALA for 24 hours. (**G**) qPCR analysis of GCLC mRNA levels in siP300 LoVo and SW-620 CSCs. (**H**) Western blot analysis was performed to assess GCLC expression in siP300 LoVo and SW-620 CSCs. (**I**) qPCR analysis of GCLC mRNA levels in shLDHA LoVo and SW-620 CSCs. (**J**) Western blot analysis was performed to assess GCLC expression

in shLDHA LoVo and SW-620 CSCs. (**K**) qPCR analysis of GCLC mRNA levels in LoVo and SW-620 CSCs cultured in regular medium containing oxamate for 24 hours. (**L**) Western blot analysis was used to assess GCLC expression in LoVo and SW-620 CSCs cultured in regular medium containing oxamate for 24 hours. (**M**) Gene expression correlation between GCLC and EP300 in TCGA-COAD and TCGA-READ datasets (n =647); R = 0.303, $p < 0.001$. (**N**) Gene expression correlation between GCLC and LDHA in TCGA-COAD and TCGA-READ datasets (n=647); R = 0.266, $p < 0.001$.

Supplemental Figure 8. **Histone lactylation defends against ferroptosis.**

(**A**) Western blot was performed to examine the expression of Pan Kla, H4K12la, GCLC, and GPX4 in SW-620 CSCs. The cells were treated with NALA (10 μM) or Ferr-1 (1 μM) along with oxaliplatin (5 μM). (**B** and **C**) Relative lipid ROS and MDA levels were tested in SW-620 CSCs treated with NALA (10 μM) or Ferr-1 (1 μM) along with oxaliplatin (5 μM) for 12 hours. (**D**) Western blot of Pan Kla, H4K12la, GCLC, and GPX4 in SW-620 CSCs treated with NALA (10 μM) or Ferr-1 (1 μM) along with oxaliplatin (5 μM). (**E** and **F**) Relative lipid ROS and MDA levels were evaluated in SW-620 CSCs treated with 2-DG (10 μM) and/or Ferr-1 (1 μM) along with oxaliplatin (5 μM) treatment for 12 hours. Three biological replicates were shown. The presented data show the mean ± SD. Comparisons were conducted using one-way ANOVA with Tukey's test. *$p < 0.05$, **$p < 0.01$, ***$p < 0.001$. ns indicates no significant difference.

Supplemental Figure 9. Inhibition of histone Lactylation suppresses GCLC function.

(**A**) Western blot analysis was used to assess the expression of GCLC, Pan Kla, H4K12la, and GPX4 in HCT-116 CSCs overexpressing GCLC and treated with

oxamate (10 mM). (**B** and **C**) Relative lipid ROS and MDA levels were assayed in HCT-116 CSCs overexpressing GCLC and treated with oxamate (10 mM) and oxaliplatin (5 μM) for 12 hours. (**D**) Western blot analysis was used to assess the expression of GCLC, Pan Kla, H4K12la, and GPX4 in HCT-116 CSCs overexpressed GCLC and treated with 2-DG (10 μM). (**E** and **F**) Relative lipid ROS and MDA levels were examined in HCT-116 CSCs overexpressed GCLC and treated with 2-DG (10 μM) plus oxaliplatin (5 μM) for 12 hours. (**G**) Western blot analysis was used to assess the expression of GCLC, Pan Kla, H4K12la, and GPX4 in LoVo CSCs overexpressing GCLC treated with or without 2-DG (10 μM). (**H** and **I**) Relative lipid ROS and MDA levels were tested in LoVo CSCs overexpressing GCLC and treated with or without 2-DG (10 μM). Cells were treated with oxaliplatin (5 μM) for 12 hours to induce ferroptosis. Three biological replicates were shown. The data represent the mean ± SD. Comparisons were conducted using one-way ANOVA with Tukey's test. *$p < 0.05$, **$p < 0.01$, ***$p < 0.001$, ****$p <0.0001$.

Supplemental Figure 10. Histone lactylation inhibits ferroptosis through GCLC. (**A**) Western blot analysis was used to assess the expression of GCLC, Pan Kla, H4K12la, and GPX4 in HCT-116 CSCs treated with NALA (10 μM) or BSO (200 μM). (**B** and **C**) Relative lipid ROS and MDA levels were measured in HCT-116 CSCs treated with oxaliplatin (5 μM) for 12 hours. (**D**) Western blot analysis was used to assess the expression of GCLC, Pan Kla, H4K12la, and GPX4 in shGCLC LoVo CSCs. (**E** and **F**) Relative lipid ROS and MDA levels were measured in LoVo CSCs treated with oxaliplatin (5 μM) for 12 hours. (**G**) Western blot analysis was performed to assess the expression of GCLC, Pan Kla, H4K12la, and GPX4 in shGCLC HCT-116 CSCs. (**H** and **I**) Relative lipid ROS and MDA levels were measured in HCT-116 CSCs treated

with oxaliplatin (5 μM) for 12 hours. (**J**) Limiting dilution assay (LDA) was performed for sphere cells injected subcutaneously into nude mice to determine tumor-initiating frequency (TIF). TIF, tumor-initiating frequency. Tumors were harvested at 42 days post implantation and represented images were taken (**J**), (**K**)tumor weights and (**L**)tumor volumes were measured in mice injected with 10,000 cells. Three biological replicates were shown. The data shown represent the mean ± SD. Comparisons were conducted using one-way ANOVA with Tukey's test. *$p < 0.05$, **$p < 0.01$, ***$p < 0.001$, ns indicates no significant difference.

Supplemental Figure 11. Enhanced chemosensitivity of drug-resistant CSCs by targeting GCLC.

(**A and B**) Cell survival was evaluated in resistant and sensitive SW-620 and LoVo CSCs treated with oxaliplatin for 24 hours. (**C** and **D**) Relative lipid ROS and MDA levels were examined in SW-620 CSCs treated with oxaliplatin (5 μM) for 12 hours. (**E**) Relative lipid ROS and MDA levels were evaluated in SW-620 and LoVo CSCs treated with oxaliplatin (5 μM) for 12 hours. (**F**) Relative lipid ROS and MDA levels were tested in LoVo CSCs treated with oxaliplatin (5 μM) for 12 hours. (**G** and **H**) Cell survival was evaluated in the resistant LoVo and SW-620 CSCs treated with oxaliplatin and/or BSO for 24 hours. **(I** and **J)** Cell survival was evaluated in resistant LoVo and SW-620 CSCs treated with BSO and oxaliplatin for 24 hours. Three biological replicates were shown. The data shown represent the mean ± SD. Comparisons were conducted using two-way ANOVA with Tukey's test and Student's two-tailed t-test. **$p < 0.01$, ***$p < 0.001$, ****$p < 0.0001$.

Supplemental Fig.1

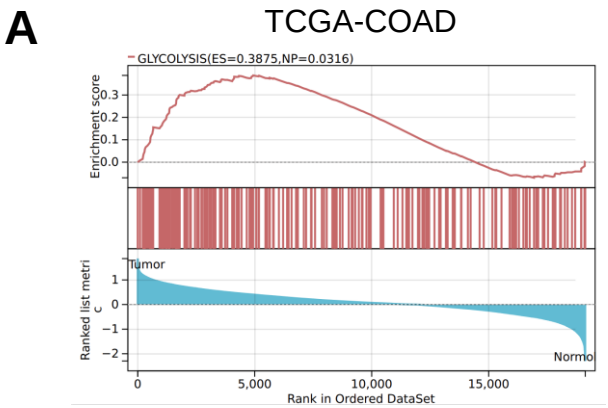

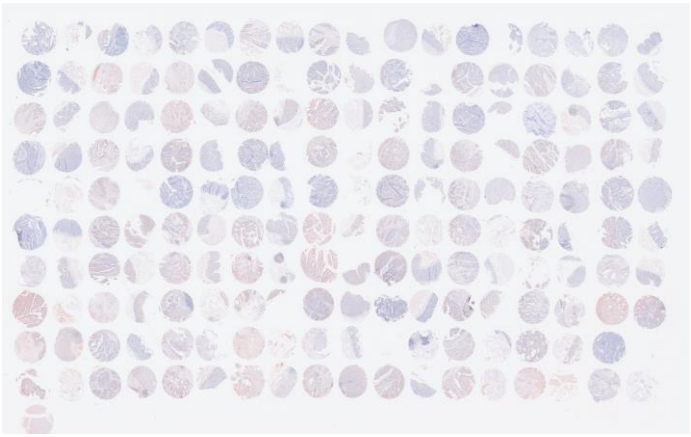

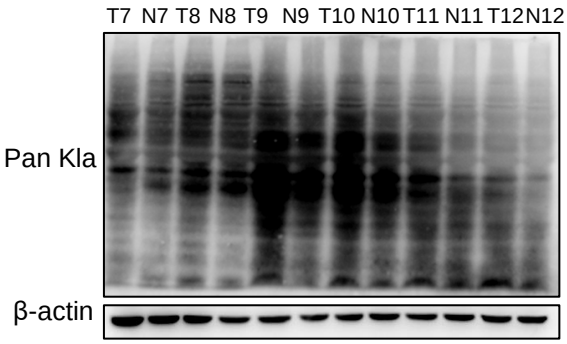

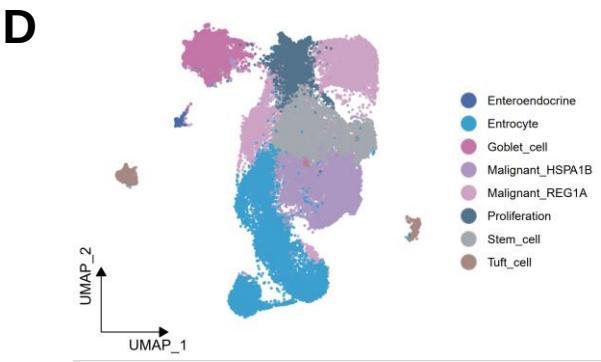

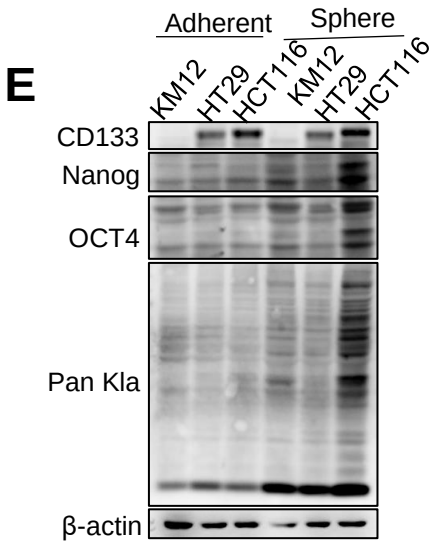

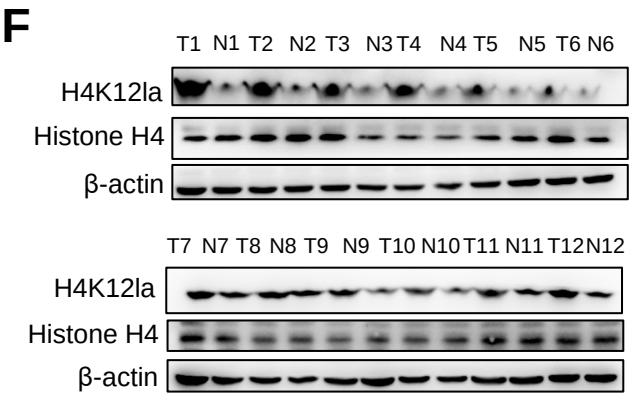

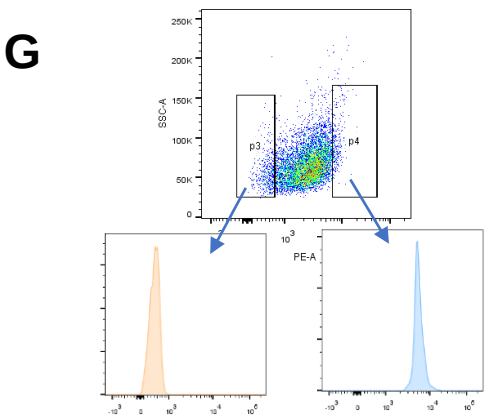

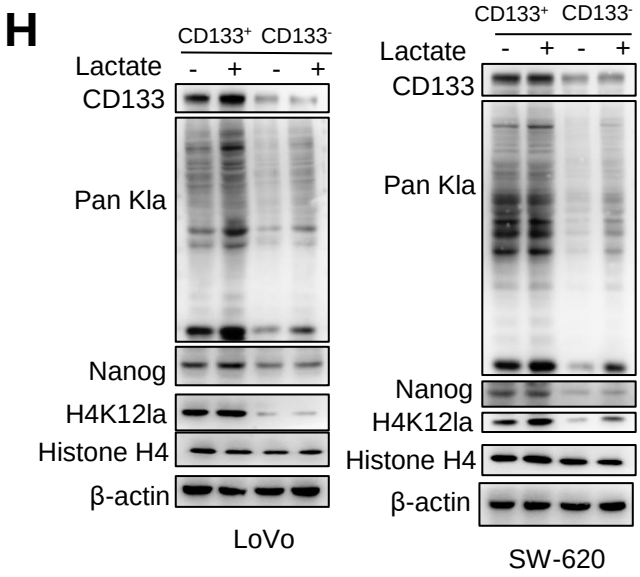

Supplemental Fig. 2

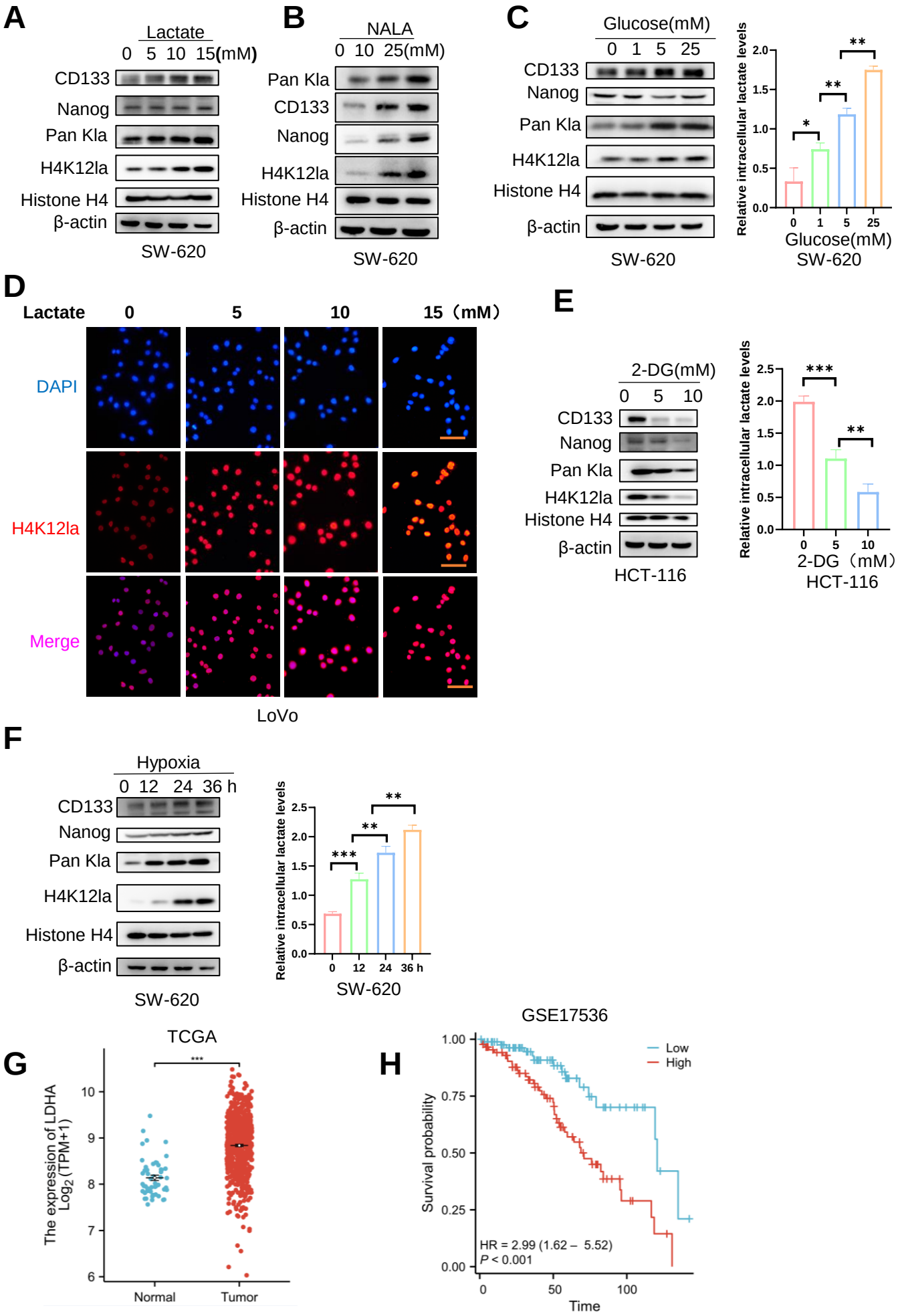

Supplemental Fig. 3

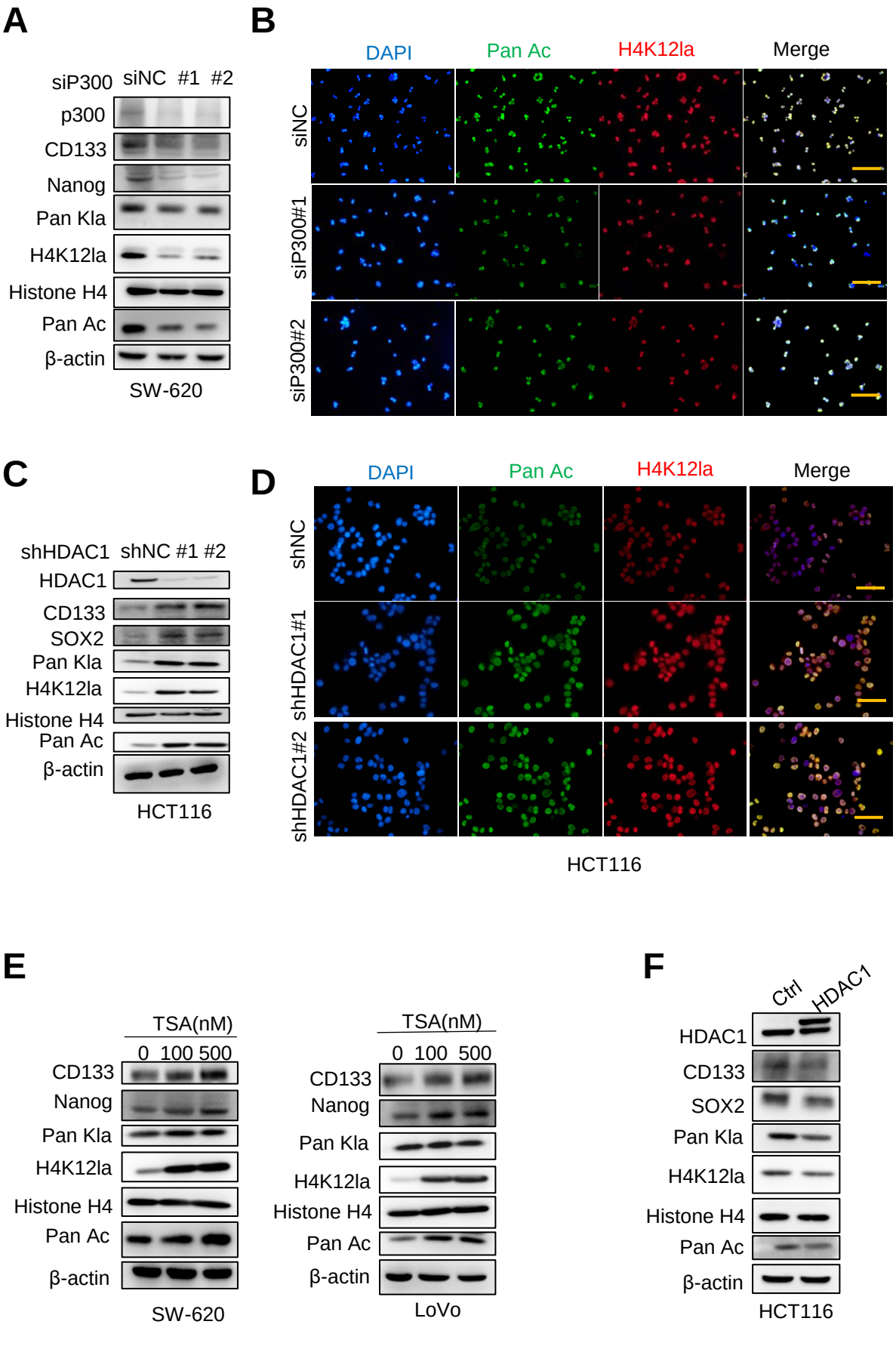

Supplemental Fig. 4

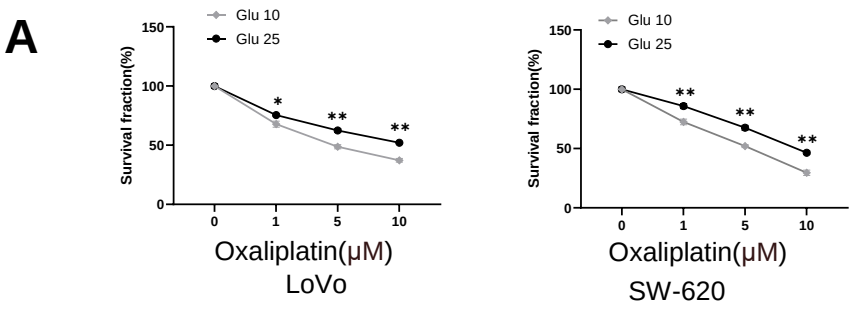

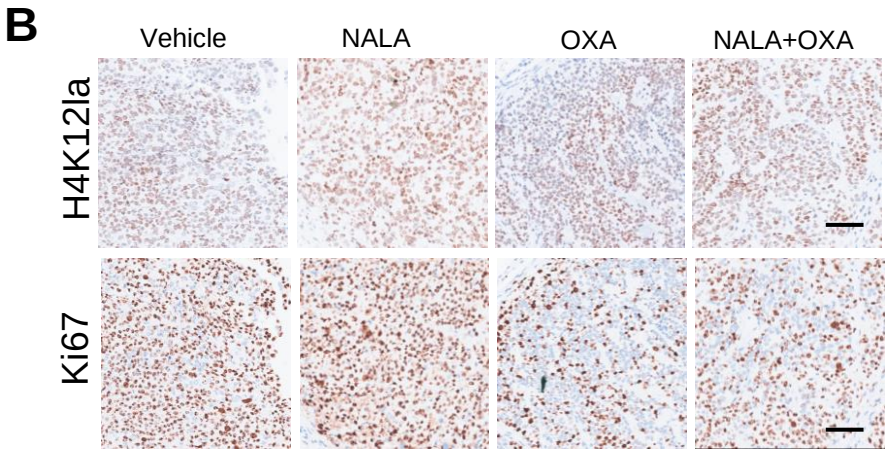

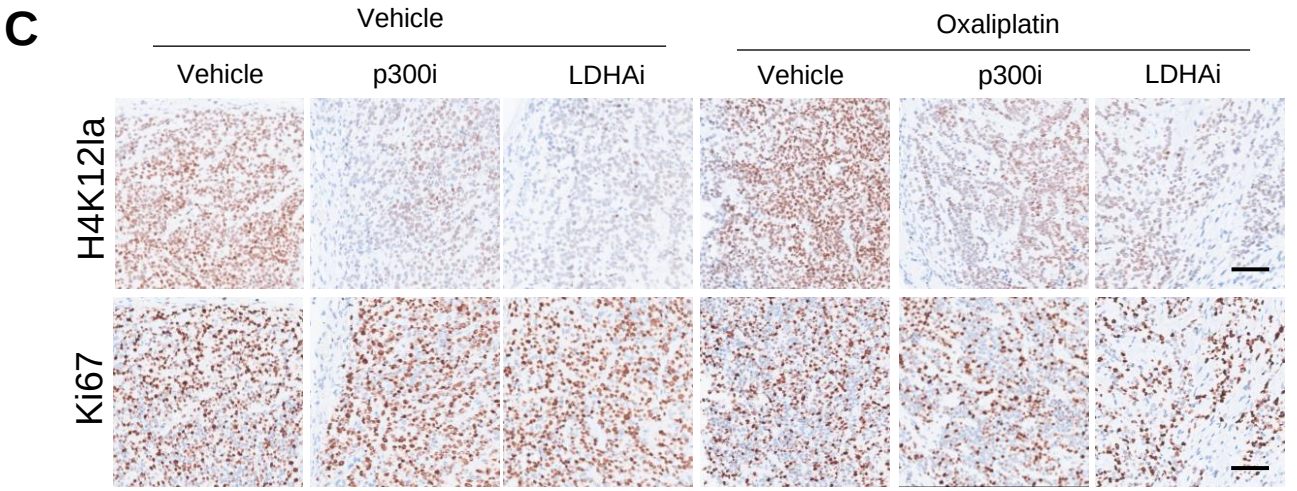

Supplemental Fig. 5

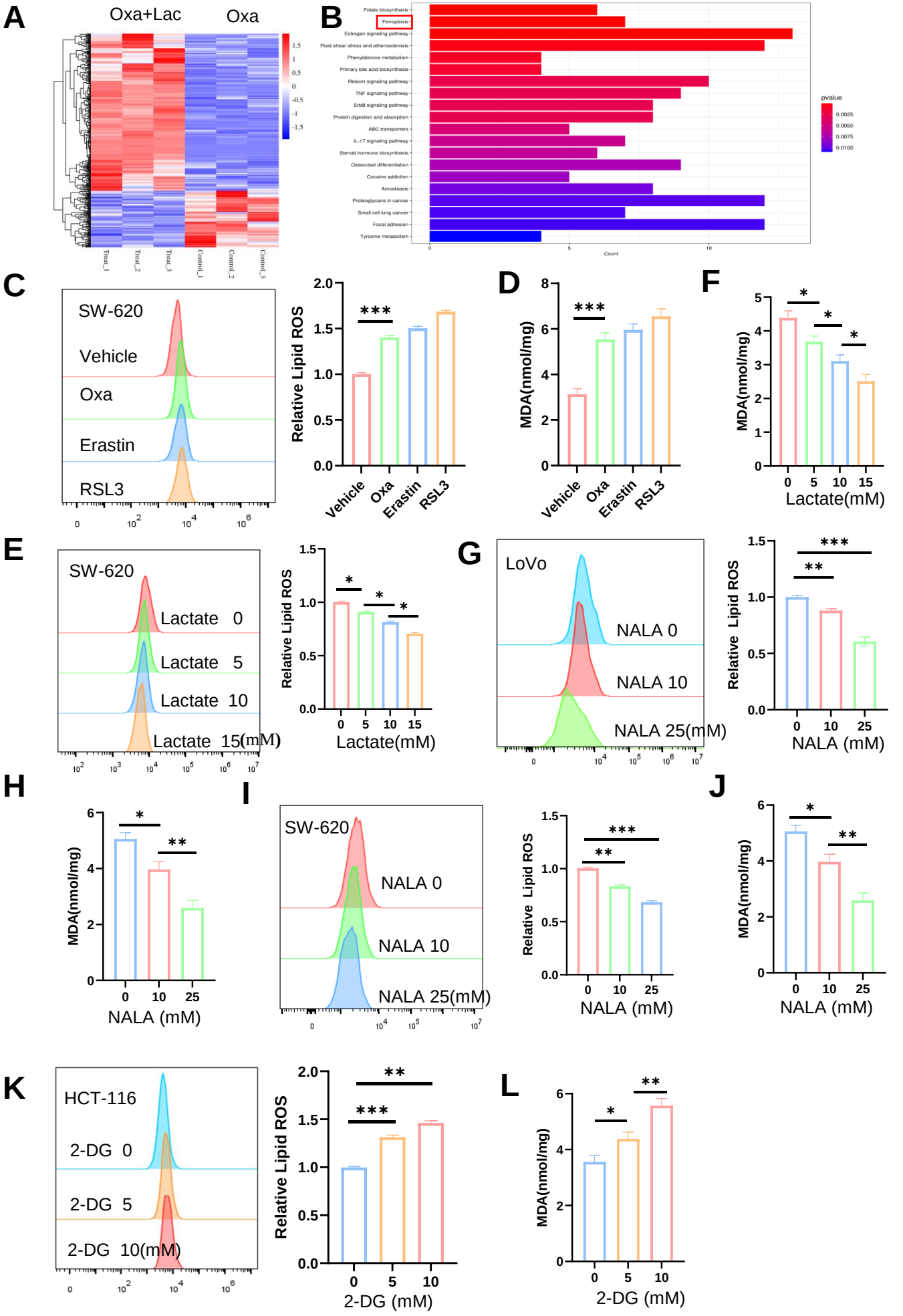

Supplemental Fig. 6

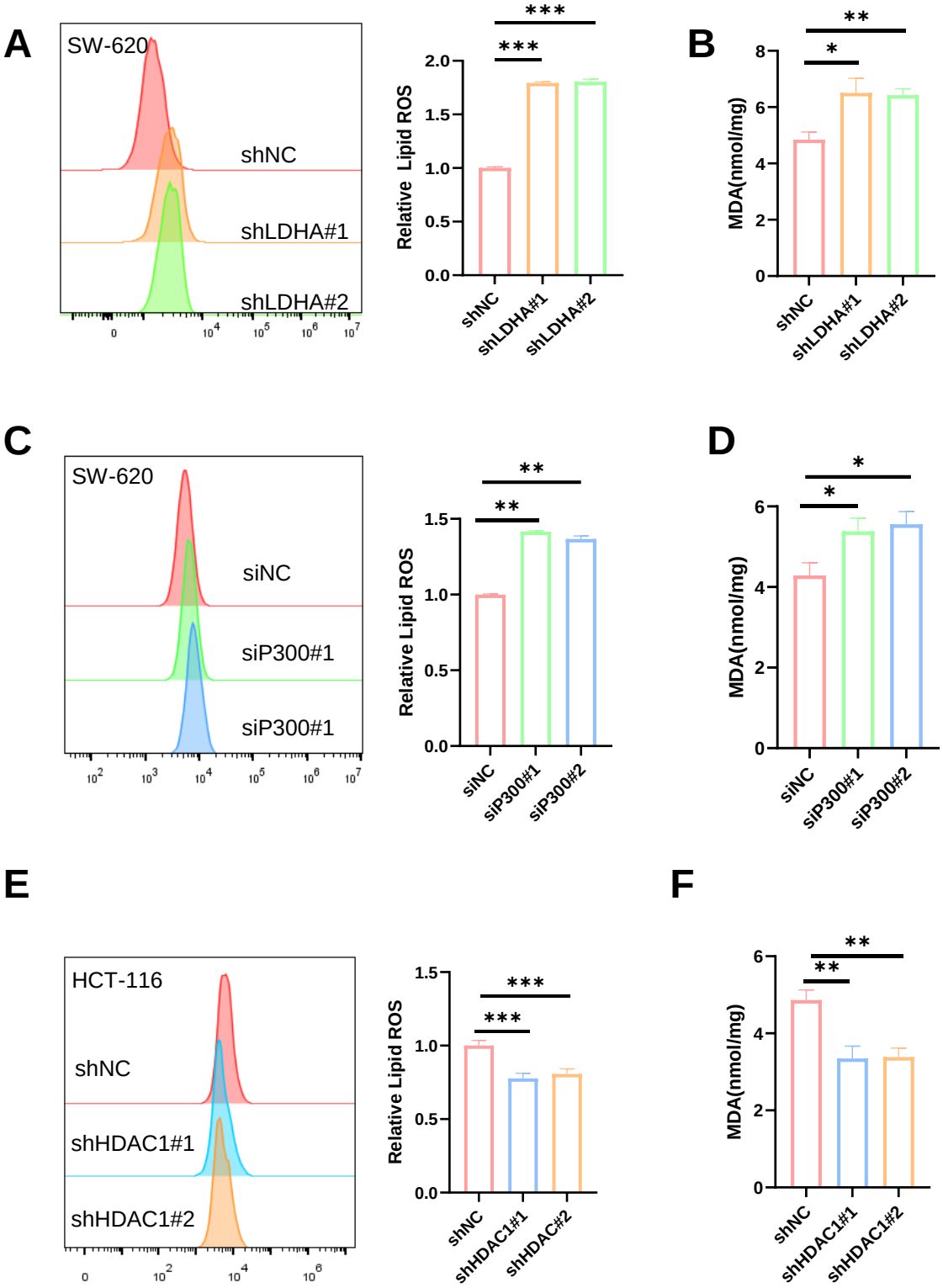

Supplemental Fig. 7

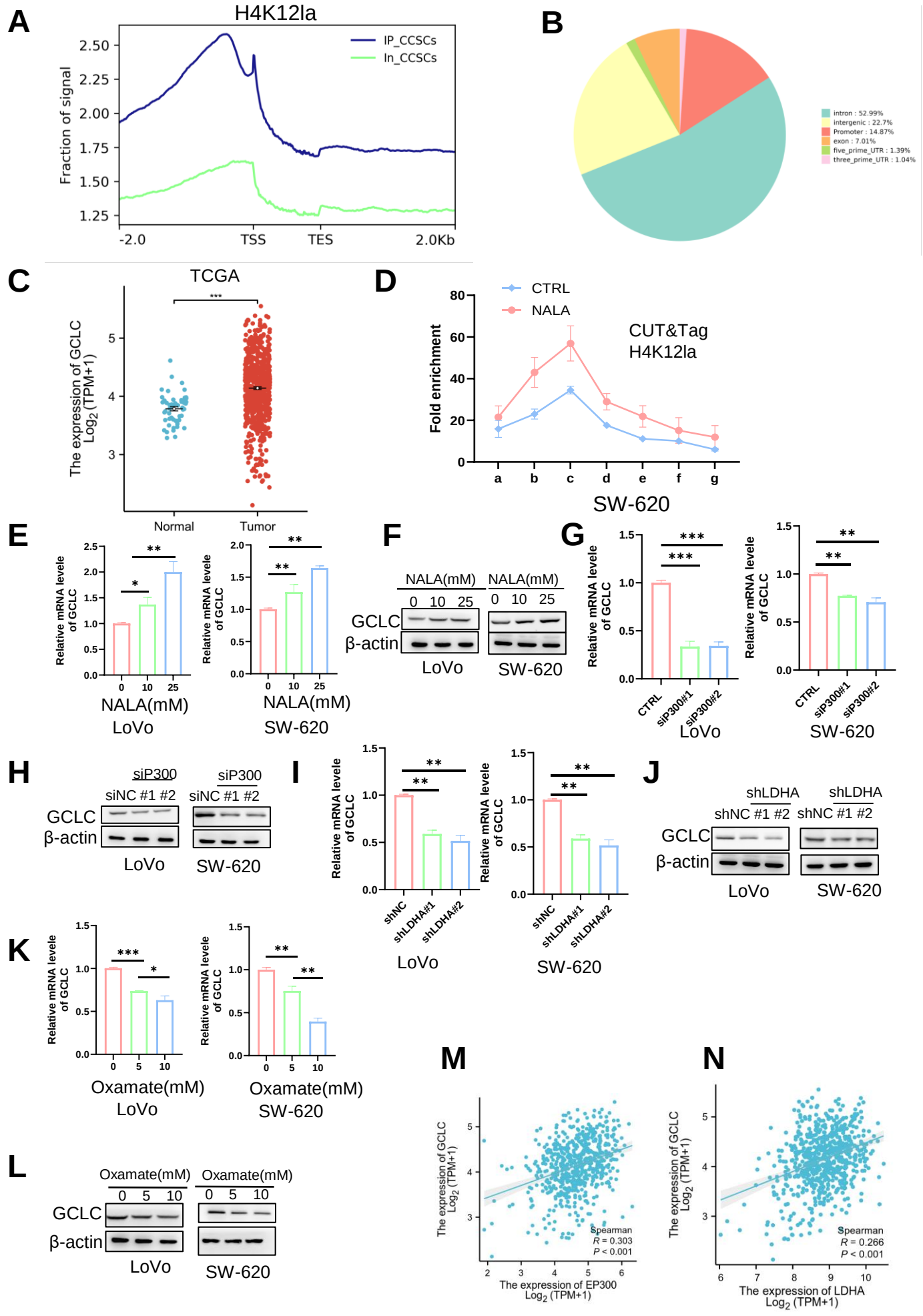

Supplemental Fig. 8

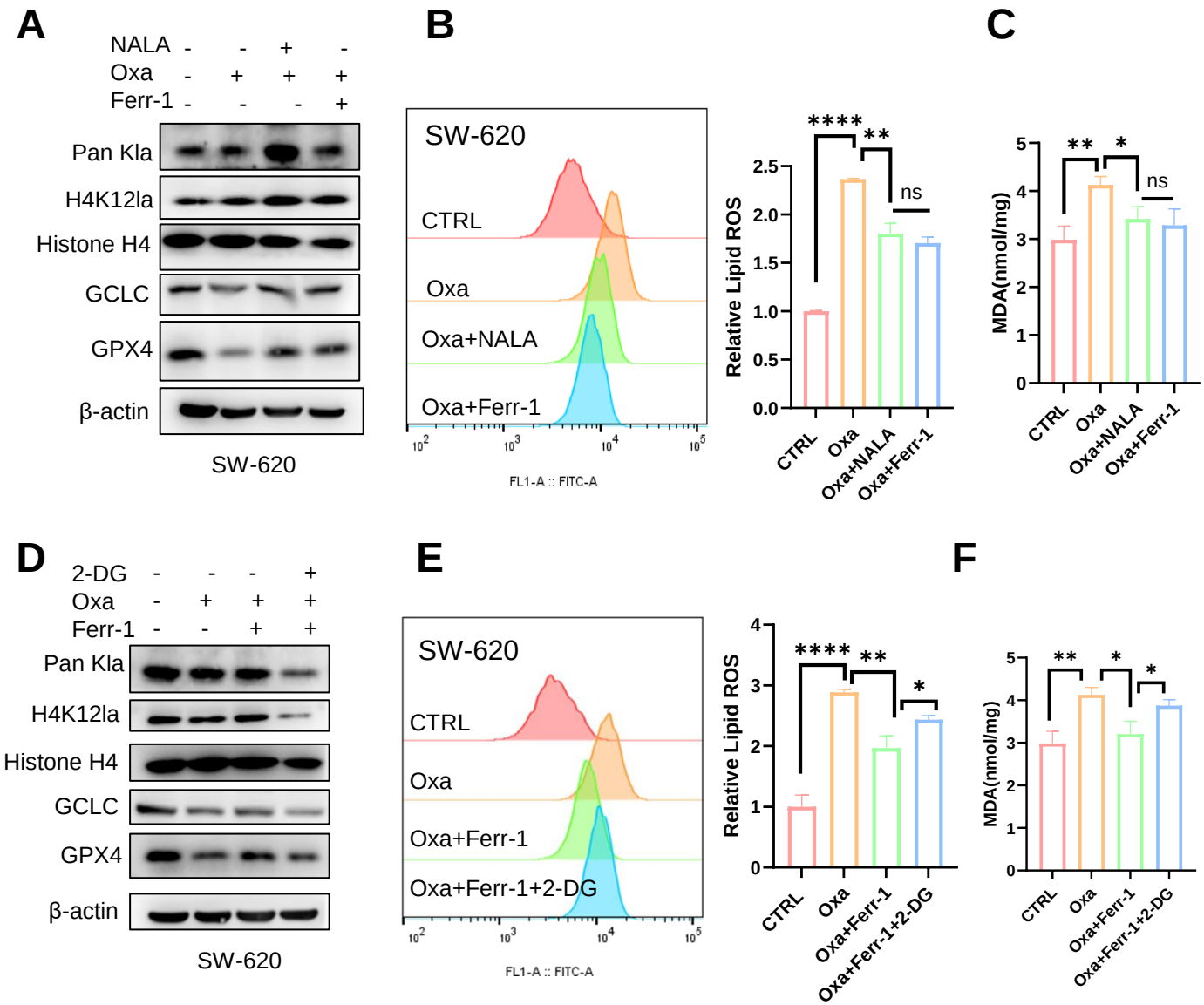

Supplemental Fig. 9

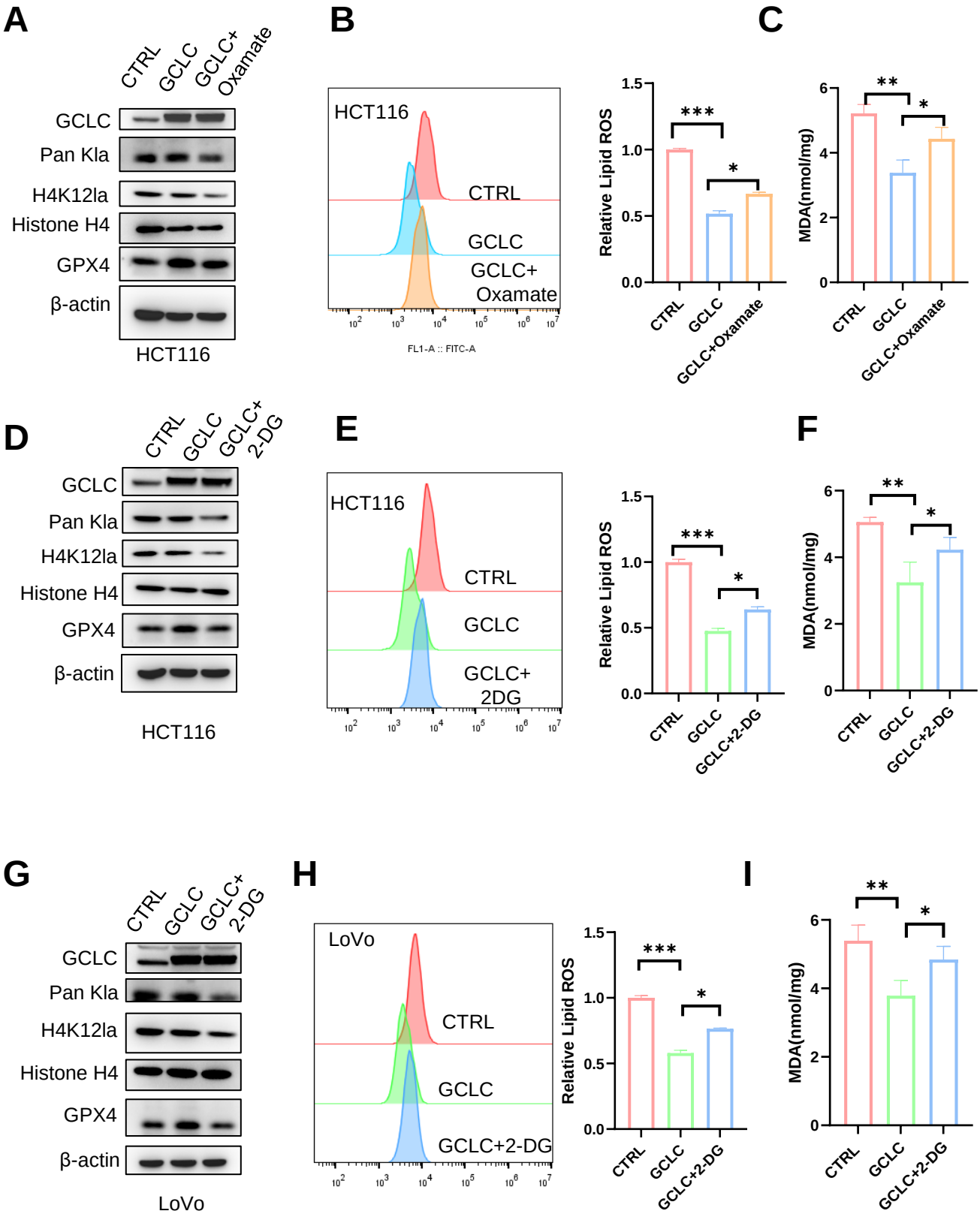

Supplemental Fig. 10

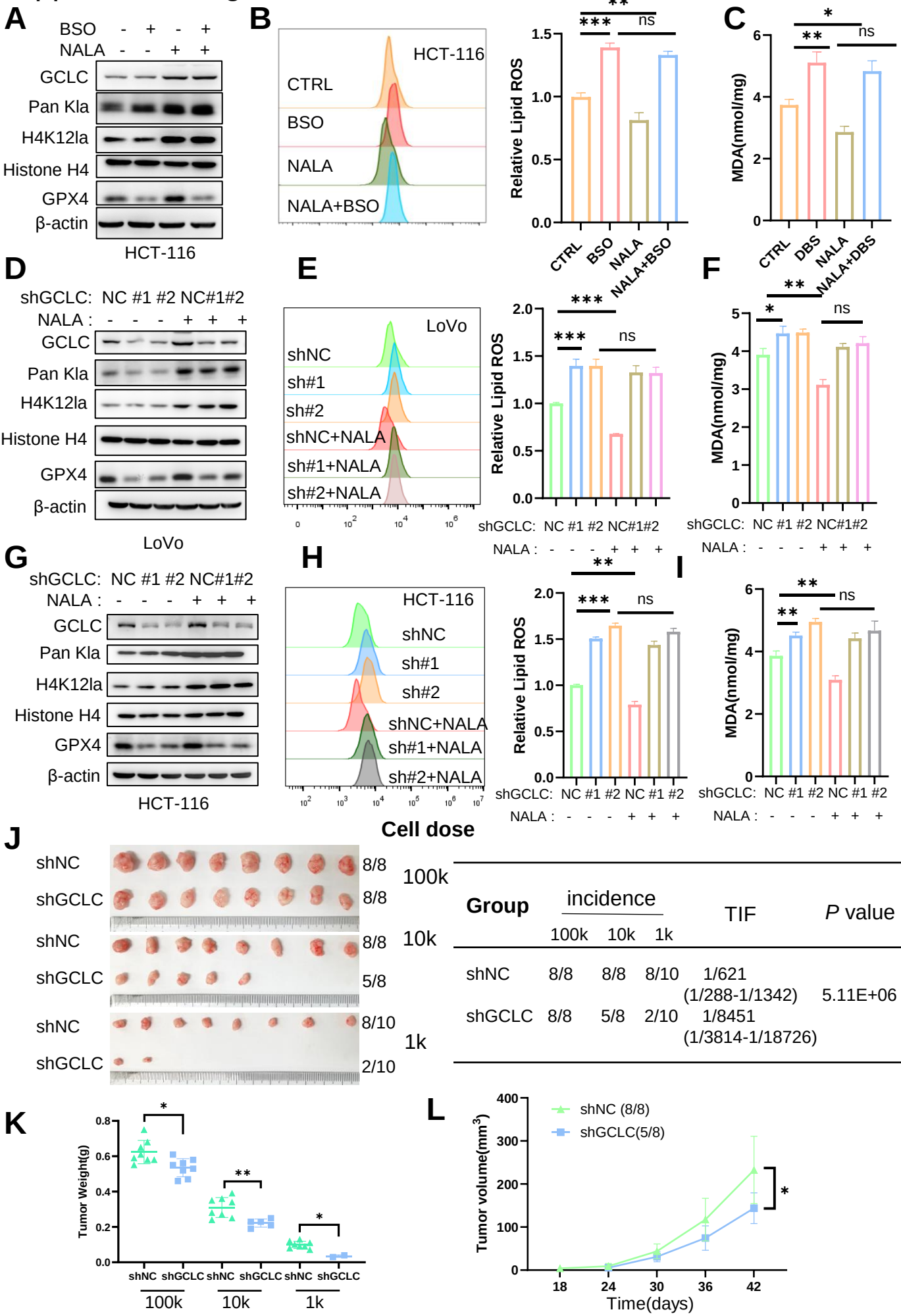

Group	incidence			TIF	*P* value
	100k	10k	1k		
shNC	8/8	8/8	8/10	1/621 (1/288-1/1342)	5.11E+06
shGCLC	8/8	5/8	2/10	1/8451 (1/3814-1/18726)	

Supplemental Fig. 11

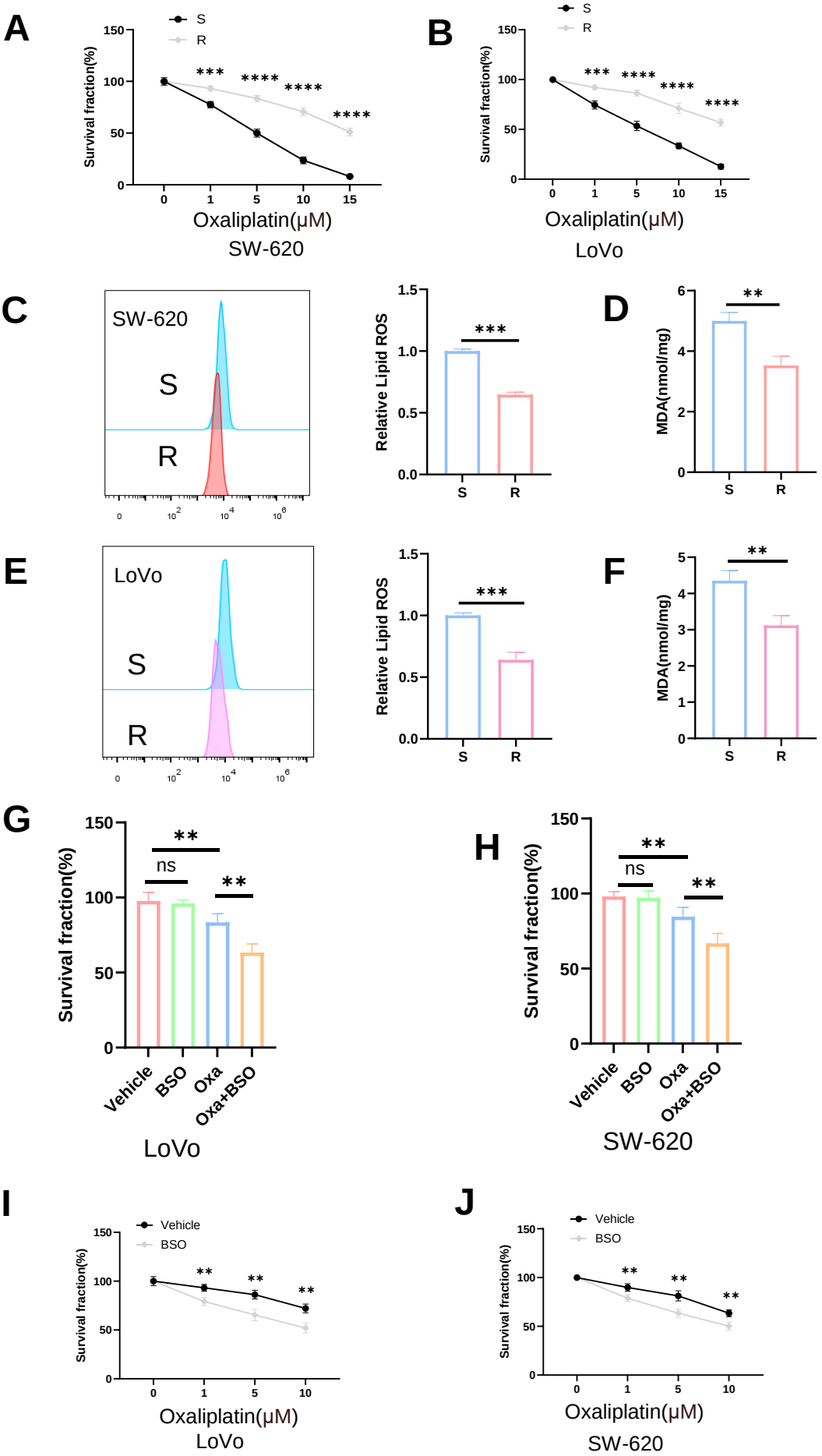

Table S1 Pan Kla binding proteins

The file is included as an excel file

Description	Score
Histone H4	63.54806781
Histone H2B	53.29506576
Histone H2A	50.1964041
Histone H2A	41.88940346
Histone H1.2	28.27578676
Histone H1.4	28.22905266
Histone H2A	25.06000197
Histone H1.5	24.78438914
Histone H1.10	15.30097985
Histone H3.1	7.717903376
Histone H3-7	5.093426466
Histone H1.0	2.533623457
CREBBP	30.54
EP300	7.63
HDAC1	5.94

Table S2 The sequence of siRNA and shRNA

The sequence of siRNA and shRNA	
Gene	Sequence
sip300#1	CAATTCCGAGACATCTTGAGA
sip300#2	GCCTTCACAATTCCGAGACAT
sip300#3	CCCGGTGAACTCTCCTATAAT
shLDHA#1	CCACCATGATTAAGGGTCTTT
shLDHA#2	CCAAAGATTGTCTCTGGCAAA
shLDHA#3	CGTTTGAAGAAGAGTGCAGAT
shGCLC#1	GCCATTGAAGAACAATAACTA
shGCLC#2	CCAATTCTGAACTCTTACCTT
shGCLC#3	CCGATGCAGTATTCTGAACTA
shHDAC1#1	GCCGGTCATGTCCAAAGTAAT
shHDAC1#2	CCGCAAGAACTCTTCCAACTT
shHDAC1#3	GCTGCTCAACTATGGTCTCTA

Table S3 The prime used to construct the plasmids

The prime used to construct the plasmids		
Plasmid	Forward Prime	Reverse Prim
GCLC	ATGGGGCTGCTGTCCCAGGG	GTTGGATGAGTCAGTTTTACTTC
HDAC1	ATGGCGCAGACGCAGGG	GGCCAACTTGACCTCCTCCTTGA

Table S4 The sequences of the primers for the qPCR

The sequences of the primers for the qPCR		
Gene	Forward Prime	Reverse Prime
GCLC	GGAGGAAACCAAGCGCCAT	CTTGACGGCGTGGTAGATGT
ACTB	CATGTACGTTGCTATCCAGGC	CTCCTTAATGTCACGCACGAT
GCLC a sit	TCTGGGGGAGGCTTCTTAGG	CCCGAAACCCATCGTGTCTG
GCLC b sit	GGGTGATTGGGTCGCAGTT	TTGCGTAAAGCGAGGCCGA
GCLC c sit	CGGGCGCTCACCTCATC	TGCACATCTACCACGCCG
GCLC d sit	CCATGGAAAGACACAAGCAAATCC	GGAACCTTCCCTTTCCTGTTTA
GCLC e sit	TTCACGAGGCTCACCTCATT	GGGTAGGCTTGTGCATTGGAT
GCLC f sit	TATCTGCGCAGCCTGTTTCT	GCCTAGTGGCTCAGATGCAA
GCLC g sit	GGCAGGGAAACGTGAAGTCTG	AAGTGGCACTACTGACTGATCCT

Table S5 The information of patients

The information of patients			
ID	Gender	Age	TNM stage
1010303147	Female	52	T3N0M0
60010144349	Female	57	T3N0M0
1009900018	male	25	T4bN0M0
60010215306	male	64	T3N0M0
1010428877	Female	64	T2N0M0
1009949519	Female	56	T3N0M0
1010442781	male	58	T2N0M0
1010535308	male	48	T3N0M0
1010485641	male	37	T3N2M0
1010376570	Female	68	T1N1M0
60010312945	Female	52	T2N1M0
1010477088	male	51	T3N0M0

Table S6 colorectal cancer tissue microarray information.

Sit location	Tissue Types	Score	Level	State of survival	survival time(month)	T	N	M	AJCC 7th edition clinical staging
A01	Tumor	5	Low	1	78	T3	N0	M0	II
A03	Tumor	1.5	Low	0	1	T2	N1b	M0	III
A05	Tumor	7	Low	0	13	T3	N0	M0	II
A07	Tumor	6	Low	1	78	T3	N0	M0	II
A09	Tumor	7	Low	1	77	T3	N2b	M0	III
A11	Tumor	7	High	0	7	T4a	N2b	M0	III
A13	Tumor	2	Low	0	22	T3	N0	M1b	IV
A15	Tumor	2	Low	1	77	T3	N0	M0	II
A17	Tumor	2.5	Low	1	77	T4a	N0	M0	II
B01	Tumor	4	Low	1	77	T3	N0	M0	II
B03	Tumor	7	Low	1	77	T3	N0	M0	II
B05	Tumor	12	High	0	44	T4a	N0	M0	II
B07	Tumor	4	Low	1	77	T2	N0	M0	I
B09	Tumor	6	Low	1	76	T3	N0	M0	II
B11	Tumor	8	High	0	38	T4a	N0	M0	II
B13	Tumor	8	High	0	13	T4b	N1b	M0	III
B15	Tumor	8	High	0	8	T4a	N0	M0	II
B17	Tumor	4	Low	1	76	T1	N0	M0	I
C01	Tumor	12	High	0	56	T4a	N2a	M0	III
C03	Tumor	8	High	0	17	T4a	N0	M1b	IV
C05	Tumor	12	High	1	76	T3	N0	M0	II
C07	Tumor	12	High	0	12	T3	N0	M0	II
C09	Tumor	5	Low	1	76	T2	N0	M0	I
C11	Tumor	8	High	0	40	T2	N0	M0	I
C13	Tumor	7	Low	0	42	T3	N1a	M0	III
C15	Tumor	null		1	76	T3	N1b	M0	III
C17	Tumor	2.5	Low	0	33	T3	N0	M0	II
D01	Tumor	5	Low	1	75	T3	N1b	M0	III
D03	Tumor	12	High	1	75	T3	N0	M0	II
D05	Tumor	9	High	0	40	T4a	N0	M0	II
D07	Tumor	5	Low	1	75	T3	N0	M0	II
D09	Tumor	5	Low	1	75	T2	N0	M0	I
D11	Tumor	8	High	0	23	T4b	N1b	M0	III
D13	Tumor	7	Low	1	75	T3	N0	M0	II
D15	Tumor	8	High	1	75	T3	N0	M0	II
D17	Tumor	6	Low	1	75	T3	N0	M0	II
E01	Tumor	null		1	75	T3	N0	M0	II
E03	Tumor	6	High	1	75	T3	N0	M0	II
E05	Tumor	2.5	Low	1	75	T3	N0	M0	II
E07	Tumor	1.5	Low	1	75	T3	N0	M0	II
E09	Tumor	5	Low	0	13	T4a	N1b	M0	III
E11	Tumor	6	Low	1	74	T3	N0	M0	II
E13	Tumor	7	Low	0	39	T4a	N1b	M0	III
E15	Tumor	2	Low	1	74	T2	N0	M0	I
E17	Tumor	6	Low	0	13	T3	N0	M0	II
F01	Tumor	1.5	Low	0	1	T3	N0	M0	II
F03	Tumor	7	Low	1	73	T3	N0	M0	II
F05	Tumor	8.5	High	1	73	T4a	N1b	M0	III
F07	Tumor	6	Low	1	73	T3	N0	M0	II
F09	Tumor	12	High	1	73	T3	N0	M0	II
F11	Tumor	8	High	1	73	T3	N0	M0	II
F13	Tumor	8	High	0	7	T3	N1a	M0	III
F15	Tumor	7.5	High	1	73	T3	N1a	M0	III
F17	Tumor	6	Low	1	73	T2	N0	M0	I
G01	Tumor	8	Low	0	16	T4b	N1b	M0	III
G03	Tumor	12	High	0	16	T4a	N2a	M1a	IV
G05	Tumor	9	High	1	72	T3	N0	M0	II
G07	Tumor	12	High	0	21	T4a	N0	M0	II
G09	Tumor	9	High	1	72	T3	N0	M0	II
G11	Tumor	6	Low	1	72	T4a	N0	M0	II
G13	Tumor	8	High	1	72	T4a	N1a	M0	III
G15	Tumor	7	Low	1	71	T3	N0	M0	II
G17	Tumor	6	Low	1	71	T3	N0	M0	II
H01	Tumor	12	High	1	71	T4a	N0	M0	II
H03	Tumor	9	High	1	71	T3	N1a	M0	III
H05	Tumor	4	Low	1	71	T2	N0	M0	I
H07	Tumor	9	High	1	71	T4a	N0	M0	II
H09	Tumor	9	High	1	71	T3	N0	M0	II
H11	Tumor	7	Low	0	0.4	T3	N2b	M0	III
H13	Tumor	6	Low	0	67	T3	N0	M0	II
H15	Tumor	6	Low	1	70	T4a	N0	M0	II
H17	Tumor	12	High	0	58	T3	N0	M0	II
I01	Tumor	6	Low	1	70	T3	N0	M0	II
I03	Tumor	5	Low	1	70	T3	N0	M0	II
I05	Tumor	6	Low	1	70	T4a	N0	M0	II
I07	Tumor	12	High	1	70	T3	N0	M0	II
I09	Tumor	5	Low	1	70	T4b	N0	M0	II
I11	Tumor	1.5	Low	0	19	T4a	N2a	M0	III
I13	Tumor	8	High	0	35	T3	N0	M0	II
I15	Tumor	8	High	1	69	T4a	N1a	M0	III
I17	Tumor	2	Low	1	69	T4a	N1b	M0	III
J01	Tumor	7.5	High	1	69	T2	N0	M0	I
J03	Tumor	8.5	High	0	42	T3	N2b	M0	III
J05	Tumor	12	High	0	19	T3	N2a	M0	III
J07	Tumor	9	High	1	69	T3	N1b	M0	III
J09	Tumor	12	High	0	15	T3	N1b	M0	III
J11	Tumor	8.5	High	0	67	T4a	N1b	M0	III
J13	Tumor	6	Low	1	69	T2	N0	M0	I
J15	Tumor	12	High	0	23	T4a	N1b	M0	III
J17	Tumor	6	Low	0	19	T3	N1a	M0	III

Table S7 colorectal cancer tissue microarray information.

Sit location	Tissue Types	Score
A16	Normal	null
B08	Normal	null
D08	Normal	null
D10	Normal	null
E04	Normal	null
E10	Normal	null
F12	Normal	null
I18	Normal	null
J18	Normal	null
A02	Normal	3
A04	Normal	1.5
A06	Normal	2
A08	Normal	1
A10	Normal	1
A12	Normal	2
A14	Normal	1
A18	Normal	1.5
B02	Normal	2
B04	Normal	2
B06	Normal	3
B10	Normal	8
B12	Normal	3
B14	Normal	2
B16	Normal	1
B18	Normal	2
C02	Normal	1.5
C04	Normal	1.5
C06	Normal	3.5
C08	Normal	3
C10	Normal	4
C12	Normal	1
C14	Normal	4
C16	Normal	3
C18	Normal	1.5
D02	Normal	2
D04	Normal	1
D06	Normal	2
D12	Normal	1
D14	Normal	6
D16	Normal	4
D18	Normal	2
E02	Normal	2
E06	Normal	1.5
E08	Normal	2
E12	Normal	1.5
E14	Normal	1
E16	Normal	2
E18	Normal	1
F02	Normal	2
F04	Normal	6
F06	Normal	2
F08	Normal	2
F10	Normal	6
F14	Normal	1.5
F16	Normal	2
F18	Normal	2
G02	Normal	4
G04	Normal	8
G06	Normal	4
G08	Normal	1
G10	Normal	4
G12	Normal	2
G14	Normal	2
G16	Normal	1.5
G18	Normal	1.5
H02	Normal	1.5
H04	Normal	4
H06	Normal	8
H08	Normal	6
H10	Normal	6
H12	Normal	2
H14	Normal	2
H16	Normal	3
H18	Normal	6
I02	Normal	6
I04	Normal	2
I06	Normal	3
I08	Normal	1.5
I10	Normal	1.5
I12	Normal	1.5
I14	Normal	1.5
I16	Normal	2
J02	Normal	1.5
J04	Normal	3
J06	Normal	2.5
J08	Normal	1.5
J10	Normal	3
J12	Normal	2
J14	Normal	1.5
J16	Normal	2

Table S8 lactylation-related genes

genes				
ACTN3	ARTN	EXT2	MDH1	SAP30
GATD1	AURKA	FAM162A	MDH2	SDC1
HAGH	B3GALT6	FBP2	ME1	SDC2
HIF1A	B3GAT1	FKBP4	ME2	SDC3
LDHA	B3GAT3	FUT8	MED24	SDHC
LDHAL6A	B3GNT3	G6PD	MERTK	SLC25A10
LDHAL6B	B4GALT1	GAL3ST1	MET	SLC25A13
LDHB	B4GALT2	GALE	MIF	SLC35A3
LDHC	B4GALT4	GALK1	MIOX	SLC37A4
LDHD	B4GALT7	GALK2	MPI	SOD1
MIR210	BIK	GAPDHS	MXI1	SOX9
MRS2	BPNT1	GCLC	NANP	SPAG4
PARK7	CACNA1H	GFPT1	NASP	SRD5A3
PER2	CAPN5	GFUS	NDST3	STC1
PFKFB2	CASP6	GLCE	NDUFV3	STC2
PNKD	CD44	GLRX	NOL3	STMN1
TIGAR	CDK1	GMPPA	NSDHL	TALDO1
TP53	CENPA	GMPPB	NT5E	TFF3
ACACB	CHPF	GNE	P4HA1	TGFA
EMB	CHPF2	GNPDA1	P4HA2	TGFBI
SLC16A1	CHST1	GOT1	PAM	TKTL1
SLC16A3	CHST12	GOT2	PAXIP1	TPBG
SLC16A7	CHST2	GPC1	PC	TPI1
SLC16A8	CHST4	GPC3	PDK3	TPST1
SLC5A12	CHST6	GPC4	PFKFB1	TXN
SLC5A8	CITED2	GPR87	PFKP	UGP2
EP300	CLDN3	GUSB	PGAM1	VCAN
CREBBP	CLDN9	GYS1	PGAM2	VEGFA
KAT5	CLN6	GYS2	PGK1	VLDLR
AARS2	COG2	HAX1	PGLS	XYLT2
AARS1	COL5A1	HDLBP	PGM2	ZNF292
KAT8	COPB2	HK2	PHKA2	
KAT7	CTH	HMMR	PKM	
ATAT1	CXCR4	HOMER1	PKP2	
ABCB6	CYB5A	HS2ST1	PLOD1	
ADORA2B	DCN	HS6ST2	PLOD2	
AGL	DDIT4	HSPA5	PMM2	
AGRN	DEPDC1	IDH1	POLR3K	
AK3	DLD	IDUA	PPFIA4	
AK4	DPYSL4	IER3	PPIA	
AKR1A1	DSC2	IGFBP3	PPP2CB	
ALDH7A1	ECD	IL13RA1	PRPS1	
ALDH9A1	EFNA3	IRS2	PSMC4	
ALDOA	EGFR	ISG20	PYGB	
ALDOB	EGLN3	KDELR3	PYGL	
ALG1	ELF3	KIF20A	QSOX1	
ANG	ENO1	KIF2A	RARS1	
ANGPTL4	ENO2	LCT	RBCK1	
ANKZF1	ERO1A	LHPP	RPE	
ARPP19	EXT1	LHX9	RRAGD	